IARJSET ISSN (O) 2393-8021, ISSN (P) 2394-1588

International Advanced Research Journal in Science, Engineering and Technology

Impact Factor 7.105 ⁜ Vol. 9, Issue 4, April 2022

DOI: 10.17148/IARJSET.2022.9468

"PARAMETRIC STUDY ON RUBBERIZED CONCRETE FILLED STEEL TUBULAR (RuCFST) STIFFENED COLUMN"

Mo. Samir Pathan[1], Deepa Raval[2]

PG Student, Applied mechanics Department, LD College of Engineering, Ahmedabad, India[1]

Assistant Professor, Applied mechanics Department, LD College of Engineering, Ahmedabad, India[2]

Abstract: Concrete filled steel tube column (CFST) is a type of composite structure which uses the advantage of both steel and concrete. The disposal of scrap tires is very difficult and causes environmental issues, hence reusing them as a construction material will be a better alternative. Previous studies shows that the use of rubber particles can enhance ductility, energy absorption capacity of concrete and the elastic behaviour of structure. It reduces the weight and natural frequency of structure so it can be used in structures subjected to vibration and seismic load. But it was found that the compressive strength and modulus of elasticity of rubberized concrete reduces in comparison to the normal concrete. However, no research has been carried out to increase the load carrying capacity of RuCFST column.

Present study investigates effect of various parameters such as shape of column (circular and square), % rubber replacement, size of vertical stiffener, No. of stiffeners on load carrying capacity and ductility of Stiffened Rubberized CFST short and slender Columns for axial loading and eccentrically loading. Effect on load carrying capacity, ductility, concrete contribution ratio, strength index and confinement index are evaluated. Results from numerical analysis are compared with empirical formula given by Eurocode-4 and Job Thomas and TN Sandeep.

Keywords: Concrete filled steel tubular column, CFST, Rubberized concrete, FEA, ABAQUS.

I. INTRODUCTION

This paper presents a numerical investigation on the ductility and strength of CFST with Rubberized Concrete (RuC), which is a composite material that mixes concrete with rubber particles, by using ABAQUS Software. This research concerns the enhancement of both ductility and strength of CFST by considering a core of RuC instead of normal concrete (NC) and by using vertical stiffener plates. Stiffener plates are intermittently tied to inner surface of steel tube.

First, a brief literature review on the topic is presented. Then numerical models of CFST and RuCFST columns are developed. A numerical study on the Stiffened Rubberized CFST short column is conducted by applying axial load and considering various parameters such as shape of column (circular and square), concrete type (NC, RuC5 and RuC15), size of vertical stiffener paper (20x2, 8x5, 30x2 and 40x2), No. of stiffeners (2,3,4 and 5). Slender Columns having slenderness ratio 15 are also modelled and parametric study is carried out considering concrete type (NC, RuC5 and RuC15), axial loading and eccentrically loading with e=20mm and without any stiffeners and with 4 no. of stiffeners.

Effect on the ultimate load carrying capacity, ductility index (DI), confinement of the concrete (CCR), strength index (SI) and concrete contribution ratio (ξ) is to be found out and graphical representation of load vs deformation as well as bar charts of parameters are to be shown. Ultimate load carrying capacity of the all model found from the software is compared with the formula given by Eurocode4 and job Thomas and TN Sandeep.

II. LITERATURE REVIEW

Abuzaid et al [1] has carried out experimental analysis of six steel tubes circular columns with different thicknesses (2.75mm, 4mm and 5mm), filled with normal (CFST) and rubberized concrete (RuCFST) by replacing 10% of fine aggregate with rubber to investigate the load capacity and ductility under compression. From material testing, it was found that the compressive strength (f'_c) and modulus of elasticity (E_c) of rubberized concrete was reduced by up to 30% compared to the normal concrete. However, the reduction in the maximum axial load capacities of the RuCFST were only 1.4% to 6.6% of the control (CFST).

A.P.C. Duarte et al [2] carried out an experimental investigation on the strength and ductility of short steel tubes infilled with rubberised concrete (RuC) and with square, rectangular and circular sections is presented. The influence of various

IARJSET ISSN (O) 2393-8021, ISSN (P) 2394-1588

International Advanced Research Journal in Science, Engineering and Technology

Impact Factor 7.105 ⁜ Vol. 9, Issue 4, April 2022

DOI: 10.17148/IARJSET.2022.9468

parameters, such as the cross-section shape, steel grade, and concrete mix (Normal concrete versus RuC), on the short column strength and ductility is analysed and discussed. The main conclusion of this research is that RuCFST short columns present higher ductility than those made of standard concrete, even though they also show lower strength. This improved ductility is noticeable in columns with circular sections, rather than in square and rectangular sections.

A.P.C. Duarte et al [3] carried out a numerical investigation on the ductility and strength of short steel tubes filled with Rubberized Concrete (RuCFST). This research concerns the enhancement of both ductility and energy absorption of CFST by considering a core of RuC instead of normal concrete (NC). Based on an experimental program conducted by the authors [2], numerical models of CFST and RuCFST columns are developed. Lower strength and stiffness, but higher ductility, of RuCFST, compared to CFST columns, were numerically observed, in agreement with the experimental data; Compressive stresses developed in the concrete core of columns with circular sections were found to be up to 60% higher than the adopted unconfined concrete strength in the case of the stockiest circular column filled with standard concrete, due to confinement effects.

Qiyun Qiao et al [4] have done push-out tests on 14 square CFSTs with shear connectors to evaluate the shear-bearing capacity of shear connectors of square concrete filled steel tube (CFST). The test results show that the ultimate bearing capacity and the elastic stiffness increase with decreasing width to thickness ratio of the steel tube, and increasing thickness, length of the steel plate and increasing concrete strength.

Job Thomas et al [5] done an experimental study to find strength and deformation characteristics of short circular Concrete-filled Steel Tube (CFST) stiffened columns. The intermittently welded vertical stiffener plates are used to strengthen the steel tubes. The stiffener plates improve the bonding between the steel tube and the concrete and also enhance the confinement in the concrete, its strength and stiffness considerably. The number of stiffeners can delay the local buckling of tubes in CFST columns. The predicted axial load-carrying capacity of the CFST columns stiffened with vertical plates using the proposed model was found to be in good agreement with the experimental data. This model can be used for the design of circular CFST columns. The proposed model can also be used for the prediction of the axial load-carrying capacity of square column.

III. FINITE ELEMENT ANALYSIS

A. Part Module

Two main types of material are considered in the proposed FE modelling: an elastoplastic steel tube and vertical steel stiffener plates; and a nonlinear compression and tension concrete infill. In this section, the details of these definitions, their assignment, and their derivation are presented.

1. Material Modelling of steel

Different stress (σ)–strain (ε) models have been used for the steel material by different researchers, including the elastic-perfectly plastic model, and the elastic-plastic model with linear hardening or multi-linear hardening. At strains of general structural interest (normally less than 5%), steel exhibits no significant strain hardening. The FE model developed in this study is used for the simulation in the following unless otherwise specified. For the elastic-plastic model with linear hardening, the strain hardening modulus (E_p) was taken as $0.005E_s$, where E_s is the steel modulus of elasticity. The selection of a σ–ε relationship of steel has negligible influence on the ultimate strength and only affects the load-deformation curve slightly in a later stage.

A σ–ε model was proposed by Tao et al.,2008 [9] for structural steel with a validity range of f_y from 200 MPa to 800 MPa. This model was used to simulate the steel material in CFST columns, which is expressed as follows

$$\sigma = \begin{cases} \varepsilon E_s & 0 \le \varepsilon < \varepsilon y \\ fy & \varepsilon y \le \varepsilon < \varepsilon p \\ fu - (fu - fy) * \left(\dfrac{\varepsilon u - \varepsilon}{\varepsilon u - \varepsilon p}\right) \text{^p} & \varepsilon p \le \varepsilon < \varepsilon u \\ fu & \varepsilon \ge \varepsilon u \end{cases}$$

in which fu is the ultimate strength; εy is the yield strain, $\varepsilon y = fy/Es$; εp is the strain at the onset of strain hardening; εu is the ultimate strain corresponding to the ultimate strength; p is the strain hardening exponent, which can be determined by

$$p = E_P \cdot \left(\frac{\varepsilon_u - \varepsilon_P}{fu - fy}\right)$$

In which Ep is the initial modulus of elasticity at the onset of strain-hardening and can be taken as $0.02Es$. εp and εu are determined using the equation below, respectively.

IARJSET ISSN (O) 2393-8021, ISSN (P) 2394-1588

International Advanced Research Journal in Science, Engineering and Technology

Impact Factor 7.105 ⁜ Vol. 9, Issue 4, April 2022

DOI: 10.17148/IARJSET.2022.9468

$$\varepsilon_p = \begin{cases} 15\varepsilon_y & fy \le 300 \\ [15 - 0.018(fy - 300)]\varepsilon u & 300 < fy \le 800 \end{cases}$$

$$\varepsilon_u = \begin{cases} 100\varepsilon_y & fy \le 300 \\ [100 - 0.15(fy - 300)]\varepsilon u & 300 < fy \le 800 \end{cases}$$

T N Sandeep and Job Thomas have done an experimental study of stiffened CFST. They have conducted a tension test on the strips taken from the steel tubes as per IS 1608 [20] and the average yield and ultimate strength were found to be 260.8 MPa and 377 MPa respectively. Modulus of elasticity of steel strip was determined and is equal to 199 GPa. The yield strength of steel plates used as stiffener was also tested and found to be 252 MPa. From the above numerical calculation, the excel spreadsheet has been generated the following stress-strain relation for steel tube as well as for vertical stiffeners is developed and shown in figure 1 (a) & 1(b).

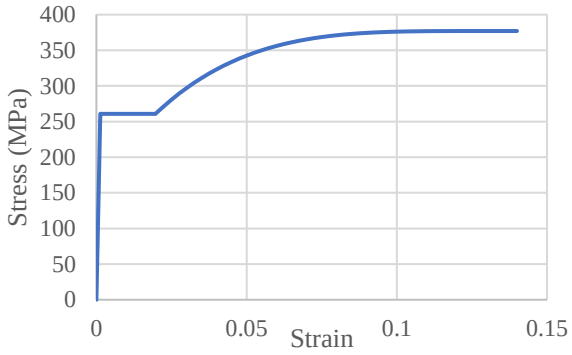

Fig. 2(a) Stress-strain relation behaviour of steel tube steel

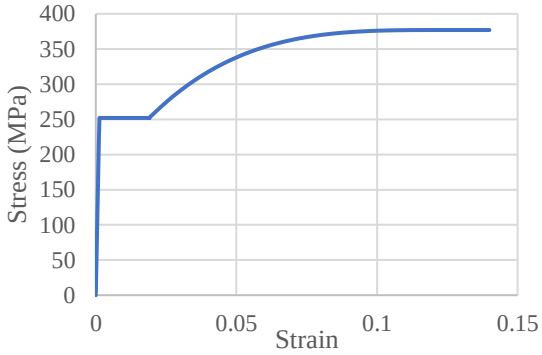

Fig. 1(b) Stress-strain relation behaviour of stiffeners

TABLE I ELASTIC MATERIAL PROPERTY OF STEEL TUBE & STIFFENER

Young's Modulus	199000 MPa
Poisson's Ratio	0.3

2. Material Modelling of concrete

The plastic behaviour of concrete was modelled using the Concrete Damaged Plasticity (CDP) model in ABAQUS [7]. The CDP model requires the definition of both the concrete's compressive and tensile stress–strain curves through the specification of tabular data (pairs of stresses-σ, strains-ε). This was performed using the appropriate commands in ABAQUS [7]. For the compressive stress–strain curves of the three concrete mixes (NC, RuC5 and RuC15), an unconfined stress–strain law was adopted comprising two parts: (i) a non-linear strain hardening (ascending) branch, until the concrete's compressive strength, f_{cm}, is reached, and (ii) a strain softening (descending) branch, as presented in figure 2 and described hereafter. It was decided to use an unconfined stress–strain law since, in this way, the confinement effects in the concrete core are included through contact (pressure) between steel and concrete. Duarte et al. [11] have done an experimental study and determined NC and RuCs properties which is shown in Table Ⅱ and the expression for non-linear behaviour provided in Eurocode 2 part 1–1 [13], which read

$$\sigma = f_{cmcyl}\frac{k\eta - \eta^2}{1 + (k-2)\eta}$$

$$\eta = \frac{\varepsilon}{\varepsilon_c}$$

$$k = 1.05E_{cm}\frac{\varepsilon}{f_{cmcy_l}}$$

where (i) $E_{cm}$is the concrete's young's modulus (Table Ⅱ), (ii) f_{cmcyl} is the equivalent cylinder concrete compressive strength and (iii) ε_c is the strain for $\sigma = f_{cmcyl}$, which depends on the concrete mix ε_c= 0.0020 for NC, ε_c= 0.0042 for RuC5 & ε_c= 0.0057 for RuC15.

Additionally, the equivalent cylinder concrete compressive strength f_{cmcyl} of the concrete mixes (NC, RuC5 and RuC15) was assessed by means of [23],

IARJSET ISSN (O) 2393-8021, ISSN (P) 2394-1588

International Advanced Research Journal in Science, Engineering and Technology

Impact Factor 7.105 ⁜ Vol. 9, Issue 4, April 2022

DOI: 10.17148/IARJSET.2022.9468

$$f_{cm_{CyL}} = \left[0.76 + 0.2\, log_{10} \frac{f_{cm}}{19.6}\right] f_{cm}$$

where f_{cm} is the average value of concrete compressive strength, experimentally determined using cubic specimens [2], presented in Table Ⅱ.

TABLE Ⅱ MECHANICAL PROPERTIES OF THE CONCRETE MIXES [8]

Concrete Mix	f_{cm} (MPa)	E_{cm} (GPa)	f_{ctm}	ε_{cm}	μ
NC	49.5	37.6	3.4	0.20	0.20
RuC5	39.3	33.4	2.6	0.42	0.21
RuC15	25.2	26.5	2.0	0.54	0.23

In the strain softening branch of the concrete compressive stress–strain law, a first approach consisted of modelling the concrete behaviour, inside both circular and square steel tubes, with a linear descending stress–strain curve. Similarly, to the procedure proposed by other authors [10,11,20,24], the slope of the descending branch was defined by a reduction factor k3=0.9, applied to the concrete equivalent compressive strength $f_{cm_{CyL}}$ at a given strain value, herein taken as εd = 0.010. Finally, as mentioned earlier, ABAQUS [15] also requires the definition of the tensile behaviour of concrete, in the CDP model, to be simulated by a softening law using the/CONCRETE TENSION STIFFENING command [7]. To do so, the experimentally determined splitting tensile strengths, f_{ctm} (Table Ⅱ) of the concrete mixes were adopted for the onset of cracking, and the tensile stress was linearly varied to zero for a corresponding ultimate cracking displacement of 0.08 mm, i.e., a fully opened crack. From the above numerical calculation, the excel spreadsheet has been generated the following stress-strain relation for Concrete mixes (NC, RuC5 and RuC15) and shown in figure 2.

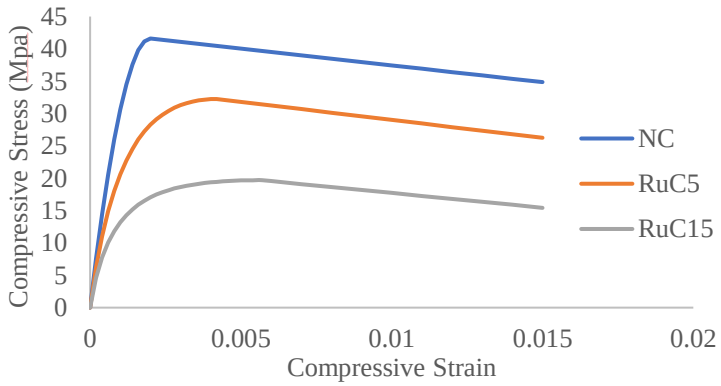

Fig. 2 Stress-strain relation behaviour of concrete core

After establishing the uniaxial stress-strain diagram for confined concrete in both compression and tension, the concrete material behaviour can then be defined in ABAQUS by defining the following two main sections:

ELASTIC: The linear segment of the confined concrete's stress-strain curve is defined in this section. The Young's modulus of concrete and the confined concrete's Poisson's ratio (μ) are defined in this part are shown in Table Ⅱ.

PLASTIC: There are several material definition algorithms provided by ABAQUS for the nonlinear behaviour of concrete materials. The concrete damage Plasticity parameters defined in this section are shown in Table Ⅲ.

TABLE Ⅲ CONCRETE DAMAGED PLASTICITY DATA

Dilation angle (ψ)		Flow potential Eccentricity (e)	Kc	fbo/fco'	Viscosity parameter
NC	20°	0.1	1.167	0.67	0
RuC5	15°				
RuC15	10°				

IARJSET ISSN (O) 2393-8021, ISSN (P) 2394-1588

International Advanced Research Journal in Science, Engineering and Technology

Impact Factor 7.105 ⁜ Vol. 9, Issue 4, April 2022

DOI: 10.17148/IARJSET.2022.9468

B. Assemble Module

The location of each part was properly set after the assembly of all three instances as shown in Figure 3. Finally, to ease the process of any later assignment certain surfaces and a set of nodes were defined in each part along with reference points.

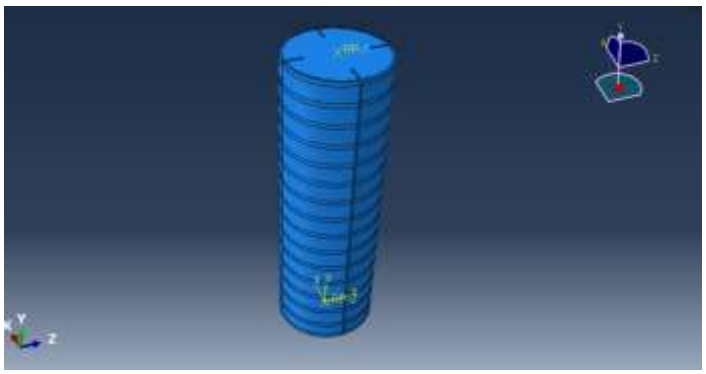

Fig. 3 Assembled section

C. Interaction Module

General contact is usually used for the interaction simulation of the steel tube and concrete. Tangent contact can be simulated by the Coulomb friction model. For CFST stub columns, there is little or no slip between the steel tube and concrete since they are loaded simultaneously. For this reason, the column's behaviour is not sensitive to the selection of friction coefficient between steel and concrete. The general bond strength is simulated through the contact friction. A coefficient of friction between them was taken as 0.25. According to X. Dai, D. Lam [6] it was found that there was little effect on the axial resistance when different friction factors were used but using a smaller friction factor induced a convergent problem with large deformation. Therefore, a friction factor of 0.2 or 0.3 is suggested to achieve a quick convergence and to obtain an accurate result.

Multi-point constraints (MPCs) allow constraints to be imposed between different degrees of freedom of the model; and can be quite general (nonlinear and nonhomogeneous). The most required constraints are available directly by choosing an MPC type and giving the associated data. MPC Beam connection provides a rigid beam between two nodes to constrain the displacement and rotation at the first node to the displacement and rotation at the second node, corresponding to the presence of a rigid beam between the two nodes. In these models, MPC Beam type connection is defined at top and bottom surface connecting all the nodes of steel and concrete to act as rigid plate. Abaqus determines the nodes to be tied using the default position tolerance. Tie connection is defined between vertical stiffeners and outer tube for a 5mm thickness and with a spacing of 24 mm. Tie connections are shown in figure 4.

D. Boundary Condition and Loading Module

The boundary condition will play a very important role to get the final failure pattern. Loading was applied to the columns by continuously imposing an upward longitudinal displacement (along Y axis) to the bottom face, while maintaining the upper face fully restrained in terms of this degree-of-freedom.

Additionally, the two transversal displacements (along axes X, Z) and all three rotations of the reference nodes of both the top and bottom face were restrained. Load is assigned to the reference point created at top.

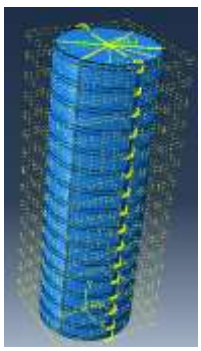

Fig. 4 Assigned Interaction

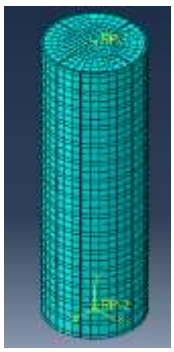

Fig. 5 Meshing of Assembly

IARJSET ISSN (O) 2393-8021, ISSN (P) 2394-1588

International Advanced Research Journal in Science, Engineering and Technology

Impact Factor 7.105 ⁜ Vol. 9, Issue 4, April 2022

DOI: 10.17148/IARJSET.2022.9468

E. Mesh Module

Both the steel tube and concrete core of the CFST were modelled using eight-node three-dimensional solid elements with reduced integration (C3D8R), with three translation degrees of freedom at each node. Mesh size is taken as 10 mm as shown in figure 5 after performing mesh convergence analysis.

IV. ANALYTICAL APPROACH

A. Eurocode 4

In this section, the ultimate strength of the tested columns is compared with the design provisions of EC4 [20] (European Standard for the design of composite steel and concrete structures – EN1994 Part 1-1 – Eurocode 4). It is well recognized that the cross-section behaviour of a given structural member is like the normal column behaviour. Prior to the evaluation of cross-section strength, EC4 [20] requires the classification of the cross-section, which is relevant to anticipate the influence of steel tube local buckling. In this study, size of the circular and square section is to be determined so that they are not under the class-4 classification according to Eurocode-4.

1. Strength of columns with square sections

The cross-section strength of a CFST column with square section can be predicted by EC4 [20] using the following design formula,

$$P_{EC4} = N_S + f_{cm_{CyL}}$$

where N_s is the axial strength of the steel tube and $f_{cm_{CyL}}$ is the equivalent cylindrical compressive strength of the concrete, which can be derived from the average value of the experimental cubic compressive strength f_{cm} using the following formula,

$$f_{cm_{CyL}} = \left[0.76 + 0.2\, log_{10} \frac{f_{cm}}{19.6}\right] f_{cm}$$

The axial strength of the steel tube is given by,

$$N_s = A_s f_y \qquad \text{for class 1; 2; 3}$$

Where As is the gross area (class 1, 2, 3) of the steel tube.

2. Strength of columns with circular sections

In the case of columns with circular section, the cross-section strength is assessed using [20],

$$P_{EC4} = \eta_a N_S + Ac\, f_{cm_{CyL}} \left(1 + \eta c \, \frac{t}{D} \frac{fy}{f_{cm_{CyL}}}\right)$$

Where all the parameters have the meaning previously described. The coefficients Ηa and Ηc account for the confinement effect provided by the circular section to the concrete core. They are given by,

$$\eta_a = 0.25(3+2\lambda_G) \leq 1.0 \qquad \eta_c = 4.9 - 18.5\,\lambda_G + 17\,(\lambda_G)^2 \geq 0$$

where $\lambda_G = (N_{pl}/N_{cr})^{0.5}$ is the global buckling slenderness of the column. It is stressed that tubes with circular section provide much higher confinement (leading to an increase of compressive strength) to the concrete core than square sections, which is a natural consequence of the revolution symmetry of circular sections. This explains the absence of coefficients Ηa and Ηc in Equation for carrying capacity of columns with square sections. Unlike tubes with square sections, which develop post-buckling strength and are characterized by higher stiffness in the corners in comparison to the central portion of the walls, tubes with circular sections do not exhibit post buckling strength but rather high imperfection sensitivity.

B. Prediction of ultimate load by J. Thomas, T.N. Sandeep

Von-Mises yield criterion is used to estimate the uniaxial stress in the steel tube and the relationship of the stresses in the von-mises criterion is given in eq. as below.

$$\sigma_{S\Theta}^2 + \sigma_{S\Theta}\sigma_{SZ} + \sigma_{SZ}^2 = \sigma_{Sy}^2$$

where $\sigma_{S\Theta}$ is the hoop stress developed in the steel tube, σ_{SZ} is the uni-axial failure stress of steel tube in the steel tube in CFST columns and σS_y is the uni-axial yield strength of steel. The confined compressive strength of concrete-filled in steel tube fcc is calculated using the method proposed by Cusson and Paultre [23] and is given by Eq.

$$f_{cc} = f_c + k f_r$$

where fc is the unconfined concrete cylinder strength, f_r is the confining pressure exerted by the steel tube on core concrete and k is the confinement efficiency factor. The magnitude of k is taken as 4.1 for steel tubes without stiffeners as proposed by Richart et al. [22]. The equilibrium of the horizontal forces is given by Eq.

$$f_r(D-2t)\, H = 2\, \sigma_{S\Theta}\, t\, H$$

IARJSET ISSN (O) 2393-8021, ISSN (P) 2394-1588

International Advanced Research Journal in Science, Engineering and Technology

Impact Factor 7.105 ⁜ Vol. 9, Issue 4, April 2022

DOI: 10.17148/IARJSET.2022.9468

where D is the outer diameter of the steel tube, t is the thickness of the tube, and H is the height of column specimen. The ultimate load of the column is the cumulative sum of the load carried by individual components such as steel tube, core concrete and stiffeners and is evidenced by,

$$N_{up} = \sigma_{SZ} A_s + f_{cc} A_c + f_{ys} A_{st}$$

where As is the area of steel tube, Ac is the area of the core concrete, Ast is the area of stiffeners, and fys is the yield strength of stiffener. Ws is the width of stiffener and n is the number of stiffeners. The relation between σSΘ, and σSy, proposed by Lai and Ho [24] is given by eq.

$$\frac{\sigma S\theta}{\sigma Sy} = \begin{cases} 0 & 0 \le \xi < 1/75 \\ 0.15\xi - 0.002 & 1/75 < \xi \le 6.68 \\ 1 & \xi \ge 6.68 \end{cases}$$

where ξ is the confinement index and is seen in Eq.

$$\xi = \frac{As\ \sigma Sy}{Ac\ fc}$$

Equation for the tri-linear relationship of the stress ratio $\sigma_{S\Theta}\sigma_{Sy}$ was developed based on the regression analysis of thirty-five experimental data by Lai and Ho [24]. The confinement offered by the steel tube in CFST columns with welded vertical stiffeners will be relatively greater than that of the columns having plain steel tubes without any stiffeners. Hence, the confinement efficiency factor proposed by Richart et al. [22] in Eq. (2) is modified to include the effect of the stiffeners. The modified confinement efficiency factor kp was developed based on the regression analysis of the test data. The confinement by the tube with stiffeners is directly proportional to the number of stiffeners n, length of the weld lw and inversely proportional to the spacing of weld s. The modified confinement efficiency factor kp is given by Eq.

$$k_p = 2.368(n\ l_w/s)$$

C. Performance indices

1. Ductility Index (DI)

The ductility index can be defined as the ratio A1/A2 as shown in figure 6, where A1 is the irrecoverable (plastic or residual) energy and A2 is the recoverable (elastic) energy at fracture.

$$DI = \frac{A1}{A2}$$

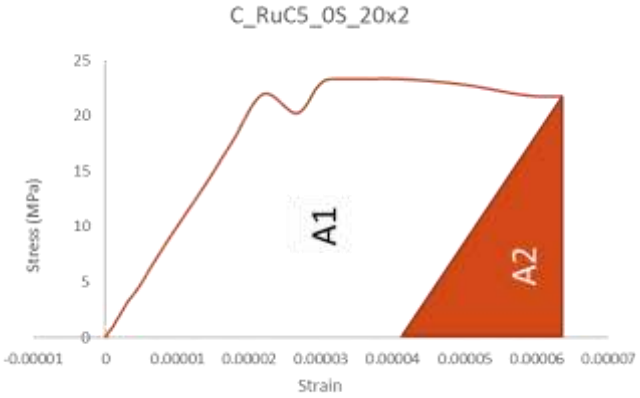

Fig. 6 Compressive Stress – strain behaviour of C_RuC5_0S_20x2 showing recoverable and irrecoverable energy

2. Strength Index (SI)

To assess the section capacity of CFSTs under concentric compression, strength index (SI) is commonly used and can be defined as follows:

$$SI = \frac{Pu}{Asfy + Ac\ fck + Ast\ fys}$$

It is defined as the ratio of the maximum compressive load-carrying capacity of the CFST column to the sum of the strength of the individual constituents.

3. Concrete Contribution Ratio (CCR)

The factor is defined as the ratio of the contribution of the ultimate load of the composite column to the ultimate load of the hollow column.

$$CCR = \frac{Pu,filled}{Pu,hollow}$$

IARJSET ISSN (O) 2393-8021, ISSN (P) 2394-1588

International Advanced Research Journal in Science, Engineering and Technology

Impact Factor 7.105 ⁜ Vol. 9, Issue 4, April 2022

DOI: 10.17148/IARJSET.2022.9468

4. Confinement Index (ξ)

The confinement effect is usually quantified by the confinement index (ξ).

$$\xi = \frac{fsAs}{(Pu - (fs\,As + Ast\,fys))}$$

V. RESULT AND DISCUSSION

A. General

This section presents the findings and outcomes of the aforesaid elaborate numerical and analytical research on stiffened RuCFST specimens. The results of ultimate load of different models with and without stiffeners also with rubber content of 5%, 15% and without any rubber content i.e., normal concrete having circular and square shape are reported. Also, the various performance indices are found and compared and load versus deformation curves for all models are found, and other parametric investigations are carried out. For a slender column of slenderness ratio of 15 and having circular shape without and with 20mm eccentricity, ultimate load is to be found.

Taking the specimen labelled C_NC_4S_20x2 as an example: (i) ‘‘C” stands for the circular cross-section shape (‘‘S” – square), (ii) ‘‘NC” stands for a normal concrete core (‘‘RuC5” –5% replacement of rubber in concrete and ‘‘RuC15” – 15% replacement of rubber in concrete), (iii) ‘‘4” is number of stiffeners and (iv) ‘‘20x2” are the nominal length and nominal thickness of stiffener in millimetres, respectively. Similarly in table 6-2, concrete mixes, no. of stiffeners and eccentricity to which loading is applied is showing. Taking the specimen labelled NC_4S_20e as an example, (i) ‘‘NC” stands for a normal concrete core (‘‘RuC5” –5% replacement of rubber in concrete and ‘‘RuC15” –15% replacement of rubber in concrete), (ii) ‘‘4” is number of stiffeners and (iii) at 20 mm loading is applied

B. Results

In the following section, the graph of applied load versus measured displacement has been plotted. Load vs longitudinal vertical displacements graphs of circular and square for vertical stiffeners of size (20x2), (30x2), (40x2) and (8x5) have been plotted and compared with theoretical formulas. The figure obtained from the finite element analysis of circular with stiffener size 20x20and 8x5 is shown in figure 7 (a) & 7 (b) below.

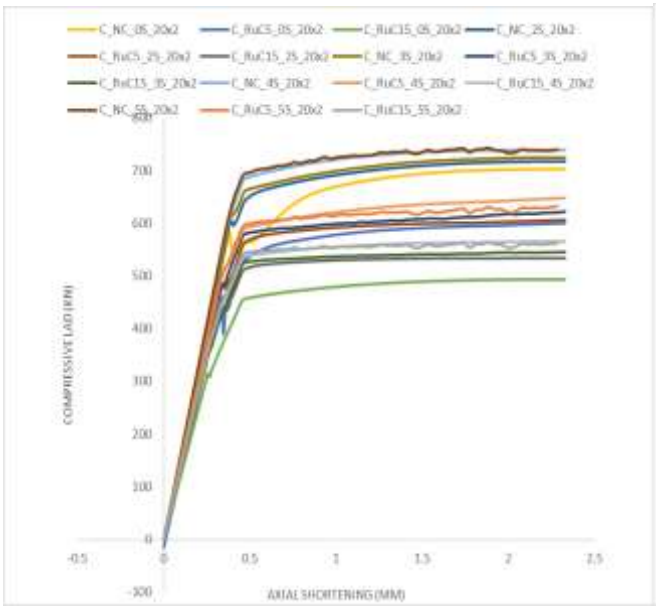

Fig. 7 (a) Axial load vs deformation graph of circular section for 20x2 size stiffeners

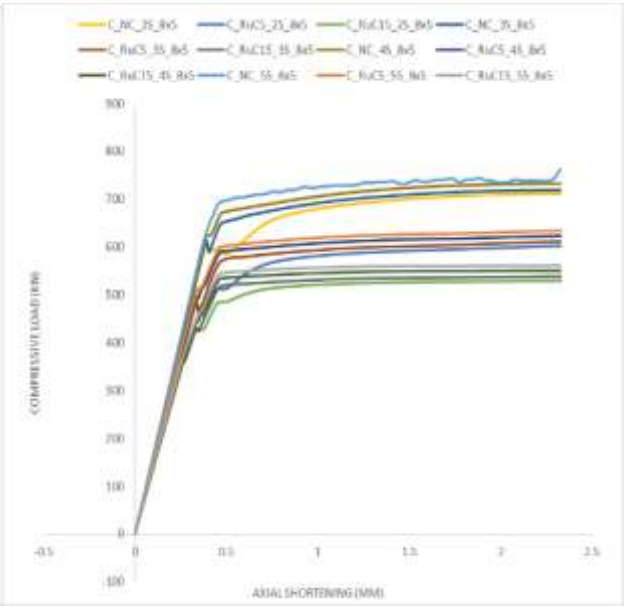

Fig. 7 (b) Axial load vs deformation graph of circular section for 8x5 size stiffeners

From the load vs displacement graphs of all the models ultimate load is to be found and is to be compared with analytical axial compression found from Eurocode-4 and from theoretical formulas given by J J Thomas and T N Sandeep shown in Table Ⅳ. Where P* = Load carrying capacity found from JJ Thomas and T N Sandeep formula; P# = Load carrying capacity found from Eurocode-4 formula. Also result from finite element analysis of slender column is shown in table V

IARJSET ISSN (O) 2393-8021, ISSN (P) 2394-1588

International Advanced Research Journal in Science, Engineering and Technology

Impact Factor 7.105 ⁜ Vol. 9, Issue 4, April 2022

DOI: 10.17148/IARJSET.2022.9468

TABLE IV RESULTS OF AXIAL COMPRESSIVE CAPACITY OF SHORT COLUMN

Sr No.	Model Name	P(FEA) KN	P* KN	P# KN
1	C_NC_0S	702.49	672.60	742.69
2	C_RuC5_0S	600.16	587.25	652.69
3	C_RuC15_0S	493.49	469.96	532.72
4	C_NC_2S_20x2	718.09	702.08	753.57
5	C_RuC5_2S_20x2	606.86	619.50	664.07
6	C_RuC15_2S_20x2	534.08	512.39	544.66
7	C_NC_3S_20x2	725.06	716.88	759.03
8	C_RuC5_3S_20x2	622.13	635.69	669.79
9	C_RuC15_3S_20x2	545.91	533.74	550.67
10	C_NC_4S_20x2	739.50	731.72	764.51
11	C_RuC5_4S_20x2	648.65	651.94	675.53
12	C_RuC15_4S_20x2	565.28	555.19	556.71
13	C_NC_5S_20x2	743.35	746.59	770.01
14	C_RuC5_5S_20x2	662.23	668.24	681.29
15	C_RuC15_5S_20x2	576.52	576.73	562.77
16	C_NC_2S_30x2	724.91	714.98	759.03
17	C_RuC5_2S_30x2	615.21	633.71	669.79
18	C_RuC15_2S_30x2	542.52	528.26	550.67
19	C_NC_2S_40x2	731.95	715.13	764.51
20	C_RuC5_2S_40x2	622.48	633.90	675.53
21	C_RuC15_2S_40x2	551.06	528.60	556.71
22	C_NC_2S_8X5	711.99	714.83	753.57
23	C_RuC5_2S_8X5	602.60	633.52	664.07
24	C_RuC15_2S_8X5	529.99	527.93	544.66
25	C_NC_3S_8X5	719.87	719.48	759.03
26	C_RuC5_3S_8X5	611.58	639.54	669.79
27	C_RuC15_3S_8X5	539.07	539.02	550.67
28	C_NC_4S_8x5	730.15	724.16	764.51
29	C_RuC5_4S_8x5	623.17	645.61	675.53
30	C_RuC15_4S_8x5	550.61	550.20	556.71
31	C_NC_5S_8x5	743.35	728.87	770.01
32	C_RuC5_5S_8x5	633.91	651.73	681.29
33	C_RuC15_5S_8X5	561.31	561.48	562.77
34	S_NC_0S_20x2	637.06	639.67	639.67
35	S_RuC5_0S_20x2	539.91	546.10	546.10
36	S_RuC15_0S_20x2	416.46	420.69	420.69

Sr No.	Model Name	P(FEA) KN	P* KN	P# KN
31	C_NC_5S_8x5	743.35	728.87	770.01
32	C_RuC5_5S_8x5	633.91	651.73	681.29
33	C_RuC15_5S_8X5	561.31	561.48	562.77
34	S_NC_0S_20x2	637.06	639.67	639.67
35	S_RuC5_0S_20x2	539.91	546.10	546.10
36	S_RuC15_0S_20x2	416.46	420.69	420.69
37	S_NC_2S_20x2	653.65	656.50	656.50
38	S_RuC5_2S_20x2	559.07	563.68	563.68
39	S_RuC15_2S_20x2	436.22	439.28	439.28
40	S_NC_3S_20x2	662.68	664.92	664.92
41	S_RuC5_3S_20x2	568.98	572.47	572.47
42	S_RuC15_3S_20x2	446.18	448.57	448.57
43	S_NC_4S_20x2	671.40	673.34	673.34
44	S_RuC5_4S_20x2	577.97	581.26	581.26
45	S_RuC15_4S_20x2	455.88	457.86	457.86
46	S_NC_4Sc_20x2	671.71	674.18	674.18
47	S_RuC5_4Sc_20x2	579.14	582.14	582.14
48	S_RuC15_4Sc_20x2	457.58	458.79	458.79
49	S_NC_2S_30x2	662.03	664.92	664.92
50	S_RuC5_2S_30x2	567.92	572.47	572.47
51	S_RuC15_2S_30x2	445.82	448.57	448.57
52	S_NC_2S_40x2	670.81	673.34	673.34
53	S_RuC5_2S_40x2	577.26	581.26	581.26
54	S_RuC15_2S_40x2	455.69	457.86	457.86
55	S_NC_2S_8x5	653.87	656.50	656.50
56	S_RuC5_2S_8x5	559.30	563.68	563.68
57	S_RuC15_2S_8x5	436.45	439.28	439.28
58	S_NC_3S_8x5	660.62	664.92	664.92
59	S_RuC5_3S_8x5	564.76	572.47	572.47
60	S_RuC15_3S_8x5	439.82	448.57	448.57
61	S_NC_4S_8x5	669.02	673.34	673.34
62	S_RuC5_4S_8x5	575.77	581.26	581.26
63	S_RuC15_4S_8x5	455.22	457.86	457.86
64	S_NC_4Sc_8x5	676.44	676.85	676.85
65	S_RuC5_4Sc_8x5	583.40	584.93	584.93
66	S_RuC15_4Sc_8x5	463.82	461.74	461.74

IARJSET ISSN (O) 2393-8021, ISSN (P) 2394-1588

International Advanced Research Journal in Science, Engineering and Technology

Impact Factor 7.105 ⁜ Vol. 9, Issue 4, April 2022

DOI: 10.17148/IARJSET.2022.9468

TABLE V RESULTS OF AXIAL COMPRESSIVE CAPACITY OF SLENDER

Sr no.	Model Name	Pu (FEA) KN
1	C_NC_0S_0e	635.692
2	C_RuC5_0S_0e	553.125
3	C_RuC15_0S_0e	442.844
4	C_NC_0S_20e	395.915
5	C_RuC5_0S_20e	350.741
6	C_RuC15_0S_20e	287.292
7	C_NC_4S_0e	664.907
8	C_RuC5_4S_0e	573.297
9	C_RuC15_4S_0e	453.557
10	C_NC_4S_20e	413.221
11	C_RuC5_4S_20e	366.564
12	C_RuC15_4S_20e	299.488

Other parameters such as ductility index (DI), strength index (SI), concrete contribution ratio (CCR) and confinement index (ξ) of each model is found from the formula as mentioned above and shown in Tabular form in table VI. An approximate cost analysis is to be carried out to have overall cost idea by using rubberized concrete and vertical stiffener plates in CFST and comparison between models is to be made. Cost of short column is shown in table VI

TABLE VI RESULTS OF PARAMETERS AND COST OF SHORT COLUMN

Sr No.	Model Name	DI	SI	CCR	ξ	Cost (Rs.)
1	C_NC_0S	3.14	0.891	2.923	0.555	216
2	C_RuC5_0S	3.8	0.887	2.552	0.716	216
3	C_RuC15_0S	3.84	0.843	2.042	1.309	216
4	C_NC_2S_20x2	4	0.894	2.818	0.608	227
5	C_RuC5_2S_20x2	4.29	0.891	2.492	0.785	227
6	C_RuC15_2S_20x2	4.55	0.85	2.077	1.436	227
7	C_NC_3S_20x2	4.28	0.896	2.775	0.635	233
8	C_RuC5_3S_20x2	4.5	0.893	2.469	0.819	233
9	C_RuC15_3S_20x2	4.84	0.853	2.098	1.499	233
10	C_NC_4S_20x2	4.38	0.897	2.736	0.662	238
11	C_RuC5_4S_20x2	4.92	0.894	2.45	0.855	238
12	C_RuC15_4S_20x2	5.13	0.856	2.122	1.564	238
13	C_NC_5S_20x2	4.5	0.899	2.702	0.69	244
14	C_RuC5_5S_20x2	5.18	0.896	2.434	0.89	244
15	C_RuC15_5S_20x2	5.52	0.859	2.148	1.629	244
16	C_NC_2S_30x2	4.1	0.896	2.755	0.635	233
17	C_RuC5_2S_30x2	4.38	0.893	2.443	0.819	233
18	C_RuC15_2S_30x2	4.68	0.853	2.05	1.499	233
19	C_NC_2S_40x2	4.31	0.897	2.696	0.662	238
20	C_RuC5_2S_40x2	4.59	0.894	2.398	0.855	238
21	C_RuC15_2S_40x2	4.97	0.856	2.026	1.564	238
22	C_NC_2S_8X5	3.07	0.894	2.818	0.608	227
23	C_RuC5_2S_8X5	3.56	0.891	2.492	0.785	227

IARJSET ISSN (O) 2393-8021, ISSN (P) 2394-1588

International Advanced Research Journal in Science, Engineering and Technology

Impact Factor 7.105 ⁜ Vol. 9, Issue 4, April 2022

DOI: 10.17148/IARJSET.2022.9468

24	C_RuC15_2S_8X5	3.62	0.85	2.077	1.436	227
25	C_NC_3S_8X5	3.33	0.896	2.775	0.635	233
26	C_RuC5_3S_8X5	3.79	0.893	2.469	0.819	233
27	C_RuC15_3S_8X5	3.89	0.853	2.098	1.499	233
28	C_NC_4S_8x5	3.95	0.897	2.736	0.662	238
29	C_RuC5_4S_8x5	4.14	0.894	2.45	0.855	238
30	C_RuC15_4S_8x5	4.38	0.856	2.122	1.564	238
31	C_NC_5S_8x5	4.06	0.899	2.702	0.69	244
32	C_RuC5_5S_8x5	4.3	0.896	2.434	0.89	244
33	C_RuC15_5S_8X5	4.54	0.859	2.148	1.629	244
34	S_NC_0S	2.12	0.89	2.86	0.538	229
35	S_RuC5_0S	2.73	0.886	2.442	0.694	229
36	S_RuC15_0S	3.28	0.841	1.788	1.269	229
37	S_NC_2S_20x2	2.72	0.893	2.692	0.591	240
38	S_RuC5_2S_20x2	3.28	0.89	2.312	0.762	240
39	S_RuC15_2S_20x2	3.35	0.848	1.717	1.395	240
40	S_NC_3S_20x2	2.8	0.895	2.619	0.618	245
41	S_RuC5_3S_20x2	3.31	0.891	2.255	0.797	245
42	S_RuC15_3S_20x2	3.5	0.851	1.686	1.459	245
43	S_NC_4S_20x2	3.24	0.897	2.551	0.645	251
44	S_RuC5_4S_20x2	3.36	0.893	2.202	0.832	251
45	S_RuC15_4S_20x2	3.87	0.854	1.657	1.523	251
46	S_NC_4Sc_20x2	3.52	0.897	2.544	0.648	251
47	S_RuC5_4Sc_20x2	3.94	0.893	2.197	0.836	251
48	S_RuC15_4Sc_20x2	4.27	0.855	1.654	1.529	251
49	S_NC_2S_30x2	2.66	0.895	2.619	0.618	245
50	S_RuC5_2S_30x2	3.04	0.891	2.255	0.797	245
51	S_RuC15_2S_30x2	3.31	0.851	1.686	1.459	245
52	S_NC_2S_40x2	3.11	0.897	2.551	0.645	251
53	S_RuC5_2S_40x2	3.27	0.893	2.202	0.832	251
54	S_RuC15_2S_40x2	3.65	0.854	1.657	1.523	251
55	S_NC_2S_8x5	2.11	0.893	2.692	0.591	240
56	S_RuC5_2S_8x5	3.13	0.89	2.312	0.762	240
57	S_RuC15_2S_8x5	3.18	0.848	1.717	1.395	240
58	S_NC_3S_8x5	2.38	0.895	2.619	0.618	245
59	S_RuC5_3S_8x5	3.24	0.891	2.255	0.797	245
60	S_RuC15_3S_8x5	3.37	0.851	1.686	1.459	245
61	S_NC_4S_8x5	3.12	0.897	2.551	0.645	251
62	S_RuC5_4S_8x5	3.3	0.893	2.202	0.832	251
63	S_RuC15_4S_8x5	3.69	0.854	1.657	1.523	251
64	S_NC_4Sc_8x5	3.37	0.897	2.524	0.656	253
65	S_RuC5_4Sc_8x5	3.66	0.894	2.181	0.847	253
66	S_RuC15_4Sc_8x5	3.9	0.856	1.645	1.55	253

IARJSET ISSN (O) 2393-8021, ISSN (P) 2394-1588

International Advanced Research Journal in Science, Engineering and Technology

Impact Factor 7.105 ⁜ Vol. 9, Issue 4, April 2022

DOI: 10.17148/IARJSET.2022.9468

From the above tables value of axial capacity from finite element analysis is taken and compared in the form of bar charts as shown in below figure 8 to 13. The effect of rubberized concrete as well as vertical stiffeners on axial load carrying capacity of RuCFST column was compared. figure 12 and 13 shows the comparison axial load capacity of slender RuCFST with and without eccentricity respectively. In below graphs yellow colour shows normal concrete, green colon shows RuC5, and red colour shows RuC15.

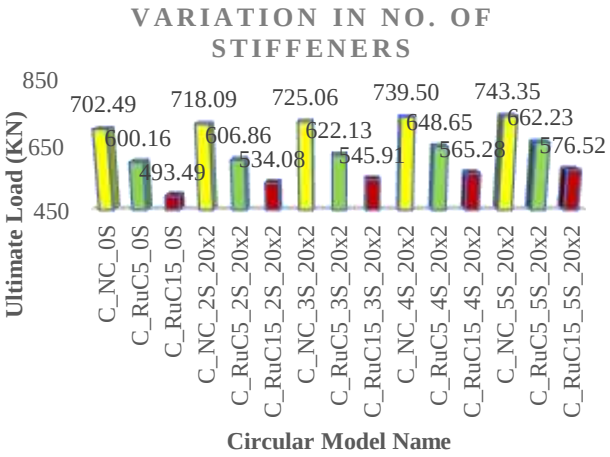

Fig. 8 Ultimate load carrying capacity by increasing no. of stiffeners of size 20x2

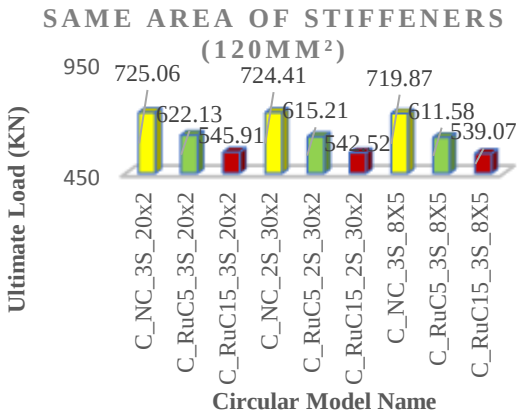

Fig. 9 Ultimate load carrying capacity by keeping same area (120mm2) of stiffeners

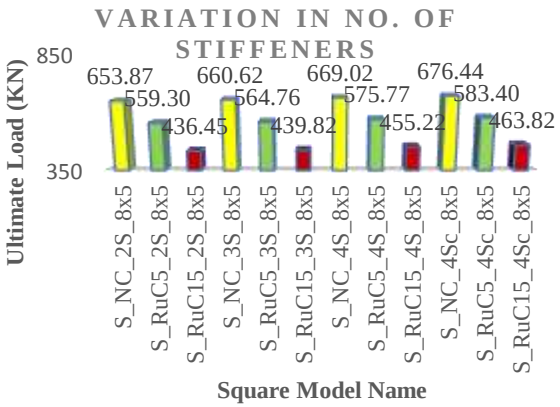

Fig.10 Ultimate load carrying capacity by increasing no. of stiffeners of size 8x5

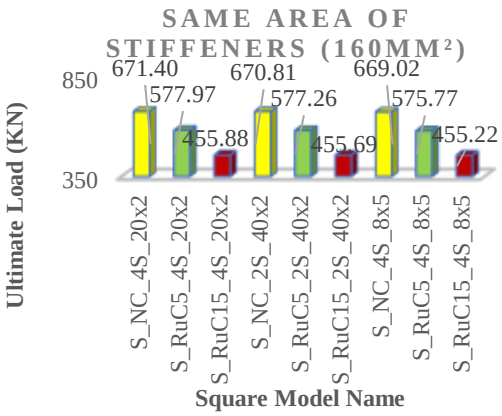

Fig.11 Ultimate load carrying capacity by keeping same area (160mm2) of stiffeners

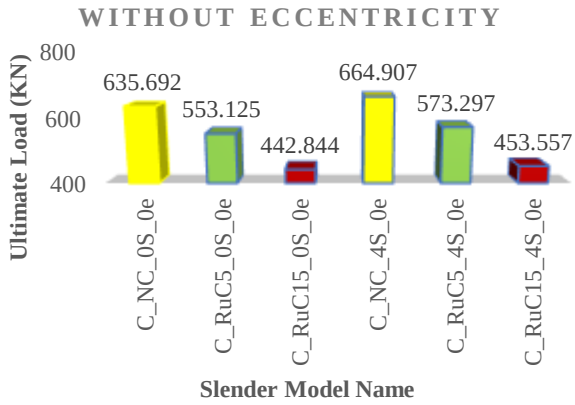

Fig.12 Ultimate load carrying capacity of slender column without eccentricity

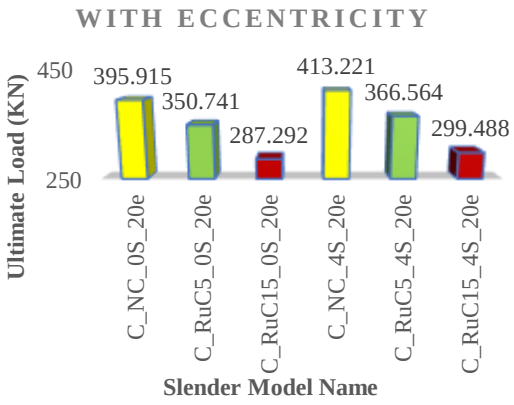

Fig.13 Ultimate load carrying capacity of slender column with eccentricity

IARJSET ISSN (O) 2393-8021, ISSN (P) 2394-1588

International Advanced Research Journal in Science, Engineering and Technology

Impact Factor 7.105 ⁜ Vol. 9, Issue 4, April 2022

DOI: 10.17148/IARJSET.2022.9468

The effect of rubberized concrete as well as vertical stiffeners on ductility index (DI), strength index (SI), concrete contribution ratio (CCR) and confinement index (ξ) of RuCFST short column was evaluated by comparing them by in form of bar graphs as shown in below figures.

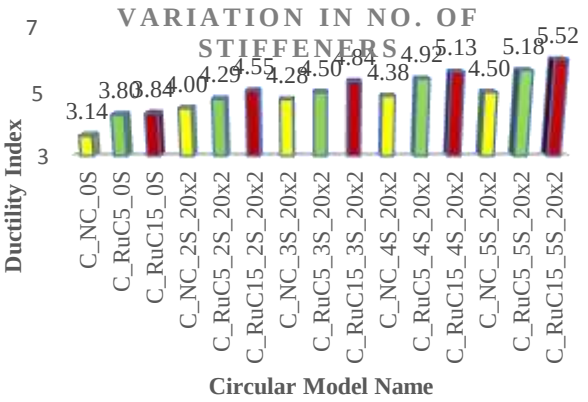

Fig.14 Ductility Index of circular column by increasing no. of stiffeners of size 20x2

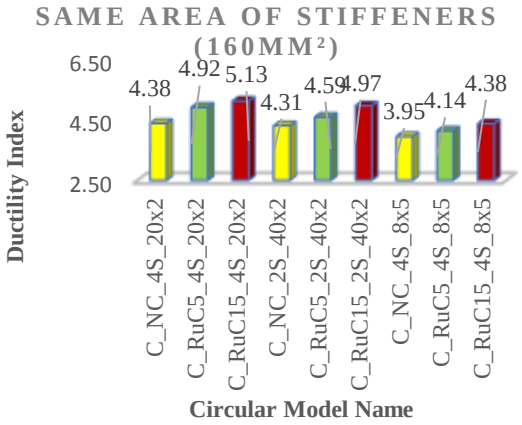

Fig.15 Ductility Index of circular column by keeping same area (160mm2) of stiffeners

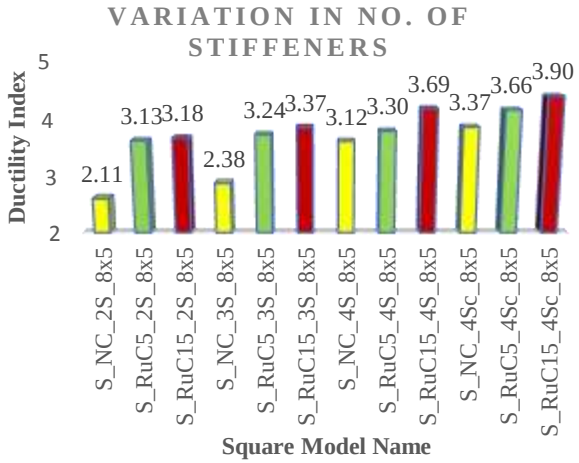

Fig.16 Ductility Index of square column by increasing no. of stiffeners of size 8x5

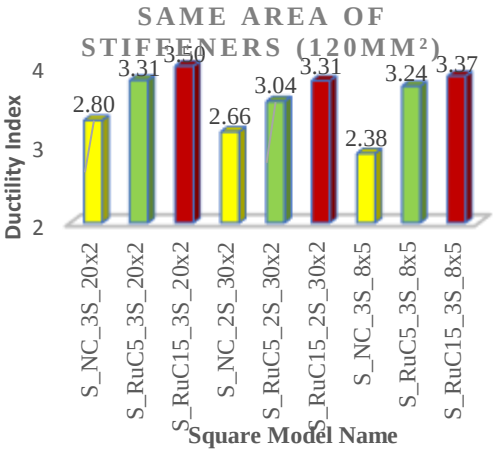

Fig.17 Ductility Index of square column by keeping same area (120mm2) of stiffeners

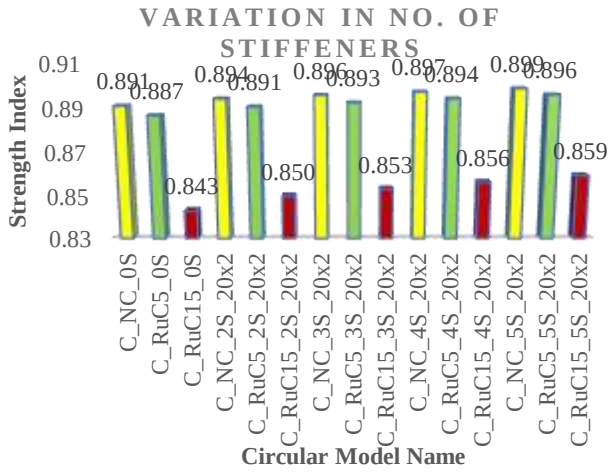

Fig.18 Strength Index of circular column by increasing no. of stiffeners of size 20x2

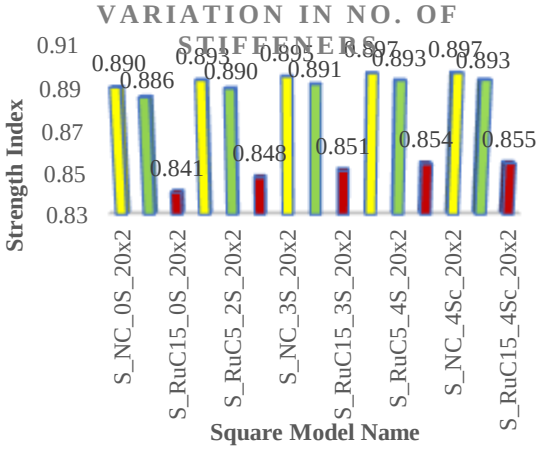

Fig.19 Strength Index of square column by increasing no. of stiffeners of size 20x2

IARJSET ISSN (O) 2393-8021, ISSN (P) 2394-1588

International Advanced Research Journal in Science, Engineering and Technology

Impact Factor 7.105 ⁜ Vol. 9, Issue 4, April 2022

DOI: 10.17148/IARJSET.2022.9468

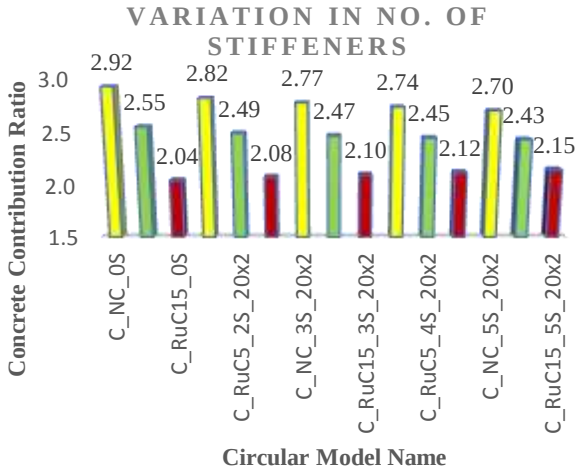

Fig.20 concrete contribution ratio of circular column by increasing no. of stiffeners of size 20x2

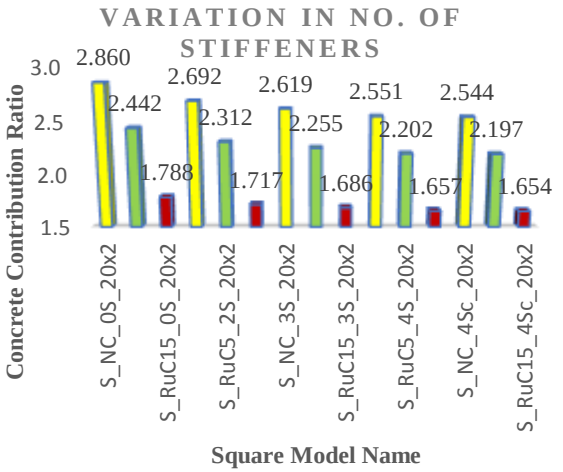

Fig.21 concrete contribution ratio of square column by increasing no. of stiffeners of size 20x2

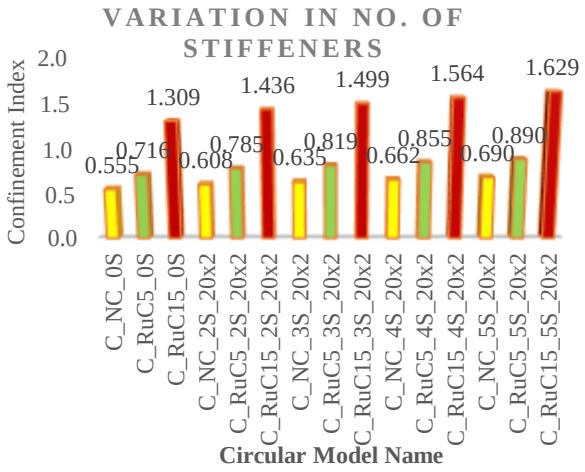

Fig.22 Confinement index of circular column by increasing no. of stiffeners of size 20x2

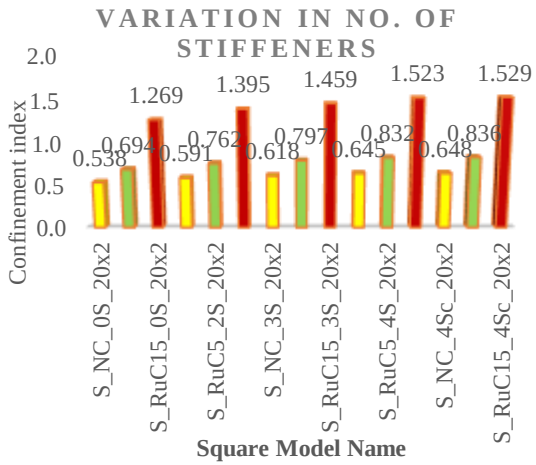

Fig.23 Confinement index of square column by increasing no. of stiffeners of size 20x2

C. Discussion

First, a brief literature review on the topic is presented. Then numerical models of CFST and RuCFST columns are developed. A numerical study on the Stiffened Rubberized CFST short column is conducted by applying axial load and considering various parameters such as shape of column (circular and square), concrete type (NC, RuC5 and RuC15), size of vertical stiffener paper (20x2, 8x5, 30x2 and 40x2), No. of stiffeners (2,3,4 and 5). Slender Columns having slenderness ratio 15 are also modelled and parametric study is carried out considering concrete type (NC, RuC5 and RuC15), pure axial loading and eccentrically loading with e=20mm and without any stiffeners and with 4 no. of stiffeners. Effect on the ultimate load carrying capacity, ductility behaviour, confinement of the concrete, strength index and concrete contribution ratio is to be found out and graphical representation of load vs deformation is to be shown. RuC mixes have lower compressive and lower young's modulus than standard concrete (NC). By increase in one number of stiffeners can lead to increase in ultimate carrying capacity up to 3 to 5%. Figure 7 (a) & (b) shows the increase in load carrying capacity as number of stiffeners increase though rubberized concrete has lower carrying capacity as compared to normal concrete. RuC15 exhibits lower axial capacity as compared to RuC15.

Bar graph for ductility index, strength index, concrete contribution ratio and confinement index are also shown in figure 8 to 23 and following points are to be noted.

- Conversely, RuC exhibits a more ductile behaviour because the RuC-to-NC Ductility index ratio increases more than 20% for 5% of rubber particles content and close to 55% for 15% of rubber particles content. Therefore, the increase

IARJSET ISSN (O) 2393-8021, ISSN (P) 2394-1588

International Advanced Research Journal in Science, Engineering and Technology

Impact Factor 7.105 ⁜ Vol. 9, Issue 4, April 2022

DOI: 10.17148/IARJSET.2022.9468

of rubber content decreases the strength and stiffness but increases the ductility of concrete. Use of stiffeners can increase load carrying capacity as well as ductility.

- For columns with square and circular sections having similar strengths, the latter shows much higher ductility than the former.
- The use of vertical stiffeners in the CFST columns enhances its strength and ductility considerably. By increase in one number of stiffeners can lead to increase in ductility index up to 8 to 20%.
- Use of RuC5 and RuC15 in circular section with 5 stiffeners instead of RuC5 and RuC15 respectively without any stiffeners can increase ultimate carrying capacity up to 9.5% and 15% and ductility index up to 25% and 30% respectively, though cost can increase up to 12%.
- Rubberized concrete shows larger confinement index. Ruc5 shows 0.5% increase in ξ though Ruc15 shows up to 5.5% increase in ξ. Square and circular CFST possess almost same ξ for same configuration though square CFST shows little, smaller value of ξ. Steel tubes with circular sections provide a more effective confinement to the concrete core.
- As no. of stiffener increases, concrete contribution ratio decreases. Which shows reduction of concrete carrying capacity to ultimate carrying capacity. Square CFST shows smaller CCR as compared to Circular CFST.
- Strength indices decrease with increase of rubber content.
- For a slender column provided with stiffeners in which load is applied without eccentrically, from going to NC to RuC15 % increase in ultimate load decrease as compared to slender column without stiffeners (4.4% for NC, 3.5% for RuC5 and 2.4% for RuC15).
- Use of 4 stiffeners in slender column result into increase in cost about 10%.
- For a slender column provided with stiffeners in which load is applied at 20mm eccentricity, as we go from NC to RuC15 % increase in ultimate load is almost same (4%) as compared to slender column without stiffeners.
- The calculation method proposed by TN Sandeep and JJ Thomas for the ultimate load carrying capacity are in good agreement with the Abaqus results.

VI. CONCLUSION AND FUTURE SCOPE

A. Conclusion

- RuC mixes have lower compressive and lower young's modulus than standard concrete (NC).
- RuC exhibits a more ductile behavior because the RuC-to-NC Ductility index ratio increases with increase in rubber particles content.
- For columns with square and circular sections having similar strengths, the latter shows much higher ductility than the former.
- Overall Cost of column increase as number of stiffeners increases with rubber or without rubber content but with the use of rubberized stiffened column load carrying capacity and ductility is largely increased.
- Strength indices decrease with increase of rubber content.
- Rubberized concrete shows larger confinement index.
- Concrete contribution ratio decreased with increase in number of stiffeners.
- As compared to short column slender column possess lower load carrying capacity which can be increased by means of stiffeners.
- Load applied with eccentricity in slender column, load carrying capacity is decreased which can be increased by use of stiffeners.

From these conclusions, a better idea of the behaviour of stiffened RuCFST columns can also be obtained. Effects of different structural parameters like DI, SI, CCR, ξ and cross-sectional shape can also be understood from this analysis, and it can be used in terms of betterment of structural systems having composite columns.

B. Future Scope

- Following are a few of the areas in which this project can be continued for the betterment of understanding the behaviour of composite columns.
- CFST columns can be prepared with different grades of concrete i.e. (M30, M40, M60, etc.), and with different percentage replacement of rubber so the effect of the grade of concrete core on the performance of the composite column can be summarized.
- Different grades of steel pipes i.e. (Fe 310, 345, or higher) can be used to confine the concrete core and their effect on the performance of the composite column can be obtained.
- The thickness of the steel pipe is an important parameter and can be kept a variable.
- Detailed experimental investigation can be carried out with Stainless steel instead of normal structural steel.
- More detailed study should be carried for slender column.
- Further eccentricity is increased, and the behaviour of the column should be analysed.

IARJSET ISSN (O) 2393-8021, ISSN (P) 2394-1588

International Advanced Research Journal in Science, Engineering and Technology

Impact Factor 7.105 ⁜ Vol. 9, Issue 4, April 2022

DOI: 10.17148/IARJSET.2022.9468

Concrete-filled steel tubes are the most advanced and effective types of composite columns. To use this column in real-life structures at a global stage, this research and other research like these can be used to develop a safer designing understanding.

REFERENCES

[1]. Abuzaid O,Nabilah A.B.,Safiee N.A. and Noor Azline M.N.,"Rubberized concrete filled steel tube", Earth and Environmental Science, 357 (2019) 012014.
[2]. A.P.C. Duarte, B.A. Silva, N. Silvestre, J. de Brito, E. Júlio, J.M. Castro, "Tests and design of short steel tubes filled with rubberised concrete",Composite Structures, Volume 274,2015.
[3]. A.P.C. Duarte, B.A. Silva, N. Silvestre, J. de Brito, E. Júlio, J.M. Castro, "Finite element modelling of short steel tubes filled with rubberized concrete",Composite Structures, Volume 150,2016.
[4]. Qiyun Qiao,Wenwen Zhang,Zhiwei Qian, Wanlin Cao, Wenchao Liu, "Experimental Study on Mechanical Behavior of Shear Connectors of Square Concrete Filled Steel Tube", Applied Science,2017
[5]. Job Thomas, T.N. Sandeep, "Capacity of short circular CFST columns with inner vertical plates welded intermittently", Journal of Constructional Steel Research, Volume 165,2020.
[6]. X. Dai, D. Lam, "Numerical modelling of the axial compressive behaviour of short concrete-filled elliptical steel columns", Journal of Constructional Steel Research, 2010.
[7]. Simulia. ABAQUS Standard, User's Manual, Version 6.10, Rhode Island, USA;2010.
[8]. L. H. Han, G. H. Yao, and Z. Tao, "Performance of concrete-filled thin-walled steel tubes under pure torsion," Thin-Walled Struct., vol. 45, no. 1, pp. 24–36, 2007.
[9]. Z. Tao, B. Uy, L. H. Han, and S. H. He, "Design of concrete-filled steel tubular members according to the Australian Standard AS 5100 model and calibration," Aust. J. Struct. Eng., vol. 8, no. 3, pp. 197–214, 2008.
[10]. Youssf O, ElGawady MA, Mills JE, Ma X, "An experimental investigation of crumb rubber concrete confined by fibre reinforced polymer tubes," Constr Build Mater 2014;53:522–32.
[11]. Duarte APC, Silva BA, Silvestre N, de Brito J, Júlio E, "Mechanical characterization of rubberized concrete using an image-processing/XFEM coupled procedure," Compos B Eng 2015;78:214–26.
[12]. IS 1608:2005, "METALLIC MATERIALS - TENSILE TESTING AT AMBIENT TEMPERATURE", Bureau of Indian Standards, New Delhi.
[13]. CEN. EN 1992-1-1, "Eurocode 2: design of concrete structures – Part 1–1: general rules and rules for buildings", Brussels, Belgium: European Committee for Standardization; 2010.
[14]. Li Z, Li F, Li JSL. "Properties of concrete incorporating rubber tyre particles", Magn Concr Res 1998;50(4):297–304.
[15]. Vermeer PA, "de Borst R. Non-associated plasticity for soils", concrete and rock. Heron 1984;29(3):3–64.
[16]. Kwasniewski M, Rodríguez-Oitabén P. "Study on the dilatancy angle of rocks in the pre-failure domain",. In: 12th ISRM international congress on rock mechanics, Harmonising Rock Engineering and the Environment, Beijing, China; 2011.
[17]. Ellobody E, Young B, Lam D. "Behaviour of normal and high strength concrete filled compact steel tube circular stub columns", J Constr Steel Res 2006;62 (7):706–15.
[18]. Ellobody E, Young B. "Nonlinear analysis of concrete-filled steel SHS and RHS columns", Thin-Walled Struct 2006;44(8):919–30.
[19]. Ellobody E, Young B, Lam D. "Behaviour of normal and high strength concrete filled compact steel tube circular stub columns", J Constr Steel Res 2006;62 (7):706–15. [11] Ellobody E, Young B. Nonlinear analysis of concrete-filled steel SHS and RHS columns. Thin-Walled Struct 2006;44(8):919–30.
[20]. CEN. EN 1994-1-1. "Eurocode 4: design of composite steel and concrete structures – Part 1-1: general rules and rules for buildings", Brussels, Belgium: European Committee for Standardization; 2004.
[21]. CEN. EN 1993-1-5. "Eurocode 3: design of steel structures – Part 1-5: plated structural elements. Brussels", Belgium: European Committee for Standardization; 2003.
[22]. F.E. Richart, A. Brandtzaeg, R.L. Brown, "A study of the failure of concrete under combined compressive stresses", Bulletin No. 185, University of Illinois, Engineering Experimental Station, 1928
[23]. D. Cusson, P. Paultre, "High-strength concrete columns confined by rectangular ties", J. Struct. Eng. 120 (3) (1994) 783e804.
[24]. M.H. Lai, J.C.M. Ho, "Behaviour of uni-axially loaded concrete-filled-steel-tube columns confined by external rings", Struct. Des. Tall Special Build. (2012)
[25]. Topçu IB. "The properties of rubberized concretes", Cem Concr Res 1995;25 (2):304–10.
[26]. Li Z, Li F, Li JSL. "Properties of concrete incorporating rubber tyre particles". Magn Concr Res 1998;50(4):297–304.

